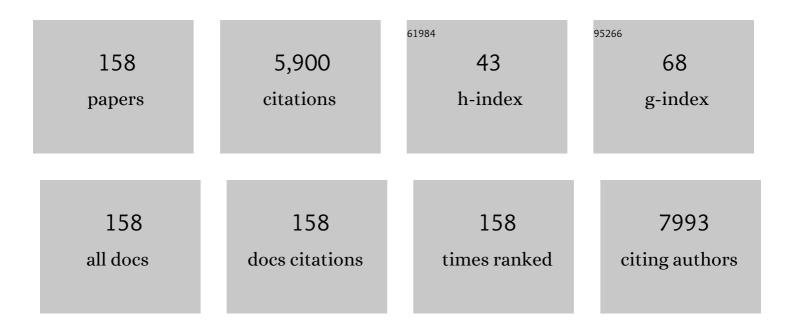
List of Publications by Year in descending order

Source: https://exaly.com/author-pdf/1987181/publications.pdf Version: 2024-02-01



<u>ΥΠΑΝΙΙΝ</u>

#	Article	IF	CITATIONS
1	Study on the Motion Stability of the Autonomous Underwater Helicopter. Journal of Marine Science and Engineering, 2022, 10, 60.	2.6	6
2	Identification of the receptor of oncolytic virus M1 as a therapeutic predictor for multiple solid tumors. Signal Transduction and Targeted Therapy, 2022, 7, 100.	17.1	17
3	Overcoming resistance to oncolytic virus M1 by targeting PI3K-γ in tumor associated myeloid cells. Molecular Therapy, 2022, , .	8.2	1
4	Insulation Degradation Analysis Due to Thermo-Mechanical Stress in Deep-Sea Oil-Filled Motors. Energies, 2022, 15, 3963.	3.1	3
5	Suppression of CCDC6 sensitizes tumor to oncolytic virus M1. Neoplasia, 2021, 23, 158-168.	5.3	8
6	Air bubbles play a role in shear thinning of non-colloidal suspensions. Physics of Fluids, 2021, 33, .	4.0	7
7	Real-Time Visualization and Quantification of Oncolytic M1 Virus <i>In Vitro</i> and <i>In Vivo</i> . Human Gene Therapy, 2021, 32, 158-165.	2.7	11
8	Surface roughness effect on the shear thinning of non-colloidal suspensions. Physics of Fluids, 2021, 33, .	4.0	7
9	Combining NanoKnife with M1 oncolytic virus enhances anticancer activity in pancreatic cancer. Cancer Letters, 2021, 502, 9-24.	7.2	30
10	Necroptotic virotherapy of oncolytic alphavirus M1 cooperated with Doxorubicin displays promising therapeutic efficacy in TNBC. Oncogene, 2021, 40, 4783-4795.	5.9	26
11	Rheology of bentonite dispersions: Role of ionic strength and solid content. Applied Clay Science, 2021, 214, 106275.	5.2	7
12	Visualization of the Oncolytic Alphavirus M1 Life Cycle in Cancer Cells. Virologica Sinica, 2021, 36, 655-666.	3.0	4
13	Oncolytic Viro-Immunotherapy: An Emerging Option in the Treatment of Gliomas. Frontiers in Immunology, 2021, 12, 721830.	4.8	50
14	Theoretical calculations and controllable synthesis of MoSe2/CdS-CdSe with highly active sites for photocatalytic hydrogen evolution. Chemical Engineering Journal, 2020, 383, 123133.	12.7	33
15	Tumors driven by <i>RAS</i> signaling harbor a natural vulnerability to oncolytic virus M1. Molecular Oncology, 2020, 14, 3153-3168.	4.6	7
16	Lonidamine potentiates the oncolytic efficiency of M1 virus independent of hexokinase 2 but via inhibition of antiviral immunity. Cancer Cell International, 2020, 20, 532.	4.1	5
17	Zinc-finger antiviral protein acts as a tumor suppressor in colorectal cancer. Oncogene, 2020, 39, 5995-6008.	5.9	12
18	Single-cell transcriptomic analysis in a mouse model deciphers cell transition states in the multistep development of esophageal cancer. Nature Communications, 2020, 11, 3715.	12.8	79

#	Article	IF	CITATIONS
19	Systematic Characterization of the Biodistribution of the Oncolytic Virus M1. Human Gene Therapy, 2020, 31, 1203-1213.	2.7	17
20	Intravenous injection of the oncolytic virus M1 awakens antitumor T cells and overcomes resistance to checkpoint blockade. Cell Death and Disease, 2020, 11, 1062.	6.3	32
21	Preparation of CdS-CoSx photocatalysts and their photocatalytic and photoelectrochemical characteristics for hydrogen production. International Journal of Hydrogen Energy, 2019, 44, 27795-27805.	7.1	26
22	An expanded landscape of human long noncoding RNA. Nucleic Acids Research, 2019, 47, 7842-7856.	14.5	92
23	Negative regulation of miRâ€1275 by H3K27me3 is critical for glial induction of glioblastoma cells. Molecular Oncology, 2019, 13, 1589-1604.	4.6	13
24	Brain activity regulates loose coupling between mitochondrial and cytosolic Ca2+ transients. Nature Communications, 2019, 10, 5277.	12.8	29
25	Rheological behavior for laponite and bentonite suspensions in shear flow. AIP Advances, 2019, 9, 125233.	1.3	9
26	Experimental Research on Seafloor Mapping and Vertical Deformation Monitoring for Gas Hydrate Zone Using Nine-Axis MEMS Sensor Tapes. IEEE Journal of Oceanic Engineering, 2019, 44, 1090-1101.	3.8	16
27	2H- and 1T- mixed phase few-layer MoS2 as a superior to Pt co-catalyst coated on TiO2 nanorod arrays for photocatalytic hydrogen evolution. Applied Catalysis B: Environmental, 2019, 241, 236-245.	20.2	242
28	SAFE-clustering: Single-cell Aggregated (from Ensemble) clustering for single-cell RNA-seq data. Bioinformatics, 2019, 35, 1269-1277.	4.1	104
29	Inhibition of the mevalonate pathway enhances cancer cell oncolysis mediated by M1 virus. Nature Communications, 2018, 9, 1524.	12.8	21
30	Intravenous injections of the oncolytic virus M1 as a novel therapy for muscle-invasive bladder cancer. Cell Death and Disease, 2018, 9, 274.	6.3	28
31	Deficiency of the IRE1α-Autophagy Axis Enhances the Antitumor Effects of the Oncolytic Virus M1. Journal of Virology, 2018, 92, .	3.4	11
32	Selective Antagonism of Bcl-xL Potentiates M1 Oncolysis by Enhancing Mitochondrial Apoptosis. Human Gene Therapy, 2018, 29, 950-961.	2.7	13
33	Dual Functional CuO _{1–<i>x</i>} Clusters for Enhanced Photocatalytic Activity and Stability of a Pt Cocatalyst in an Overall Water-Splitting Reaction. ACS Sustainable Chemistry and Engineering, 2018, 6, 17340-17351.	6.7	15
34	DNA-PK inhibition synergizes with oncolytic virus M1 by inhibiting antiviral response and potentiating DNA damage. Nature Communications, 2018, 9, 4342.	12.8	38
35	CCGD-ESCC: A Comprehensive Database for Genetic Variants Associated with Esophageal Squamous Cell Carcinoma in Chinese Population. Genomics, Proteomics and Bioinformatics, 2018, 16, 262-268.	6.9	17
36	Genotype imputation for Han Chinese population using Haplotype Reference Consortium as reference. Human Genetics, 2018, 137, 431-436.	3.8	15

#	Article	IF	CITATIONS
37	Revealing the Relationship between Photocatalytic Properties and Structure Characteristics of TiO ₂ Reduced by Hydrogen and Carbon Monoxide Treatment. ChemSusChem, 2018, 11, 2766-2775.	6.8	40
38	The Anti-Warburg Effect Elicited by the cAMP-PGC1α Pathway Drives Differentiation of Glioblastoma Cells into Astrocytes. Cell Reports, 2017, 18, 468-481.	6.4	85
39	Selective replication of oncolytic virus M1 results in a bystander killing effect that is potentiated by Smac mimetics. Proceedings of the National Academy of Sciences of the United States of America, 2017, 114, 201701002.	7.1	33
40	Targeting VCP enhances anticancer activity of oncolytic virus M1 in hepatocellular carcinoma. Science Translational Medicine, 2017, 9, .	12.4	55
41	In-situ photo-deposition CuO1â^' cluster on TiO2 for enhanced photocatalytic H2-production activity. International Journal of Hydrogen Energy, 2017, 42, 19942-19950.	7.1	38
42	Naturally Existing Oncolytic Virus M1 Is Nonpathogenic for the Nonhuman Primates After Multiple Rounds of Repeated Intravenous Injections. Human Gene Therapy, 2016, 27, 700-711.	2.7	37
43	Cyclophilin D regulates mitochondrial flashes and metabolism in cardiac myocytes. Journal of Molecular and Cellular Cardiology, 2016, 91, 63-71.	1.9	29
44	Controlled optical properties of water-soluble CdTe nanocrystals via anion exchange. Journal of Colloid and Interface Science, 2016, 463, 69-74.	9.4	7
45	Activation of Cyclic Adenosine Monophosphate Pathway Increases the Sensitivity of Cancer Cells to the Oncolytic Virus M1. Molecular Therapy, 2016, 24, 156-165.	8.2	35
46	A classical PKA inhibitor increases the oncolytic effect of M1 virus via activation of exchange protein directly activated by cAMP 1. Oncotarget, 2016, 7, 48443-48455.	1.8	23
47	Rectification and tunneling effects enabled by Al2O3 atomic layer deposited on back contact of CdTe solar cells. Applied Physics Letters, 2015, 107, .	3.3	27
48	Transcriptional upregulation of microtubule-associated protein 2 is involved in the protein kinase A-induced decrease in the invasiveness of glioma cells. Neuro-Oncology, 2015, 17, 1578-1588.	1.2	21
49	How to Optimize the Interface between Photosensitizers and TiO ₂ Nanocrystals with Molecular Engineering to Enhance Performances of Dye-Sensitized Solar Cells?. ACS Applied Materials & Interfaces, 2015, 7, 25341-25351.	8.0	28
50	Metal and F dual-doping to synchronously improve electron transport rate and lifetime for TiO ₂ photoanode to enhance dye-sensitized solar cells performances. Journal of Materials Chemistry A, 2015, 3, 5692-5700.	10.3	29
51	Double dye cubic-sensitized solar cell based on Förster resonant energy transfer. RSC Advances, 2015, 5, 10026-10032.	3.6	7
52	Kinetics Tuning of Li-Ion Diffusion in Layered Li(Ni _{<i>x</i>} Mn _{<i>y</i>} Co _{<i>z</i>})O ₂ . Journal of the American Chemical Society, 2015, 137, 8364-8367.	13.7	292
53	Prelithiation Activates Li(Ni _{0.5} Mn _{0.3} Co _{0.2})O ₂ for High Capacity and Excellent Cycling Stability. Nano Letters, 2015, 15, 5590-5596.	9.1	68
54	Effects of Ga doping and hollow structure on the band-structures and photovoltaic properties of SnO ₂ photoanode dye-sensitized solar cells. RSC Advances, 2015, 5, 93765-93772.	3.6	10

#	Article	IF	CITATIONS
55	Large-field high-resolution two-photon digital scanned light-sheet microscopy. Cell Research, 2015, 25, 254-257.	12.0	67
56	Cyclometalated ruthenium(<scp>ii</scp>) complexes with bis(benzimidazolyl)benzene for dye-sensitized solar cells. RSC Advances, 2015, 5, 90001-90009.	3.6	15
57	Janus Solid–Liquid Interface Enabling Ultrahigh Charging and Discharging Rate for Advanced Lithium-Ion Batteries. Nano Letters, 2015, 15, 6102-6109.	9.1	90
58	Enhancing the performance of dye-sensitized solar cells: doping SnO ₂ photoanodes with Al to simultaneously improve conduction band and electron lifetime. Journal of Materials Chemistry A, 2015, 3, 3066-3073.	10.3	51
59	Enhanced performance of CdTe quantum dot sensitized solar cell via anion exchanges. Journal of Power Sources, 2015, 277, 215-221.	7.8	67
60	Mitoflash frequency in early adulthood predicts lifespan in Caenorhabditis elegans. Nature, 2014, 508, 128-132.	27.8	121
61	An Increase in Conversion Efficiency of Dye-Sensitized Solar Cells using Bamboo-Type TiO2 Nanotube Arrays. Electrochimica Acta, 2014, 116, 26-30.	5.2	22
62	Effect of TiO2 nanotubes lateral spacing on photovoltaic properties of dye-sensitized solar cells. Science Bulletin, 2014, 59, 4735-4740.	1.7	0
63	Enhanced Performance of Dye-Sensitized Solar Cells By Tuning the Structure of the Photoanode Film. Electrochimica Acta, 2014, 145, 286-290.	5.2	4
64	Novel organic sensitizers containing dithiafulvenyl units as additional donors for efficient dye-sensitized solar cells. RSC Advances, 2014, 4, 34896.	3.6	29
65	Identification and characterization of alphavirus M1 as a selective oncolytic virus targeting ZAP-defective human cancers. Proceedings of the National Academy of Sciences of the United States of America, 2014, 111, E4504-12.	7.1	118
66	TiO2 compact layer for dye-sensitized SnO2 nanocrystalline thin film. Electrochimica Acta, 2014, 147, 366-370.	5.2	29
67	Pre-synthesized monodisperse PbS quantum dots sensitized solar cells. Electrochimica Acta, 2014, 144, 71-75.	5.2	13
68	Facile fabrication of highly porous photoanode at low temperature for all-plastic dye-sensitized solar cells with quasi-solid state electrolyte. Journal of Power Sources, 2014, 271, 8-15.	7.8	10
69	Mn3O4/graphene composite as counter electrode in dye-sensitized solar cells. RSC Advances, 2014, 4, 15091.	3.6	50
70	Two-Step Electrochemical Synthesis of Polypyrrole/Reduced Graphene Oxide Composites as Efficient Pt-Free Counter Electrode for Plastic Dye-Sensitized Solar Cells. ACS Applied Materials & Interfaces, 2014, 6, 16249-16256.	8.0	59
71	Preparation of monodispersed PbS quantum dots on nanoporous semiconductor thin film by two-phase method. Journal of Alloys and Compounds, 2014, 595, 51-54.	5.5	8
72	An ionic liquidâ€based polymer with Ï€â€stacked structure as allâ€solidâ€state electrolyte for efficient dyeâ€sensitized solar cells. Journal of Applied Polymer Science, 2013, 127, 2574-2580.	2.6	8

#	Article	IF	CITATIONS
73	Influence of Sn source on the performance of dye-sensitized solar cells based on Sn-doped TiO2 photoanodes: A strategy for choosing an appropriate doping source. Electrochimica Acta, 2013, 107, 473-480.	5.2	39
74	Facile Synthesis of Poly(3,4-ethylenedioxythiophene) Film via Solid-State Polymerization as High-Performance Pt-Free Counter Electrodes for Plastic Dye-Sensitized Solar Cells. ACS Applied Materials & Interfaces, 2013, 5, 8423-8429.	8.0	68
75	Plastic dye-sensitized solar cells with enhanced performance prepared from a printable TiO2 paste. Electrochemistry Communications, 2013, 34, 254-257.	4.7	21
76	Enhanced conversion efficiency of dye-sensitized titanium dioxide solar cells by Ca-doping. Journal of Alloys and Compounds, 2013, 548, 161-165.	5.5	25
77	Novel organic dye employing dithiafulvenyl-substituted arylamine hybrid donor unit for dye-sensitized solar cells. Organic Electronics, 2013, 14, 2132-2138.	2.6	32
78	The effect of oligo-organosiloxane on poly(ethylene oxide) electrolyte system for solid dye sensitized solar cells. Electrochimica Acta, 2013, 89, 29-34.	5.2	6
79	TiO2 flowers and spheres for ionic liquid electrolytes based dye-sensitized solar cells. Electrochimica Acta, 2013, 87, 629-636.	5.2	25
80	Controllable synthesis of anatase TiO2 crystals for high-performance dye-sensitized solar cells. Journal of Materials Chemistry A, 2013, 1, 5347.	10.3	29
81	Improved photovoltaic performance of dye-sensitized solar cells (DSSCs) by Zn+Mg co-doped TiO2 electrode. Electrochimica Acta, 2013, 95, 48-53.	5.2	46
82	Influence of VB group doped TiO2 on photovoltaic performance of dye-sensitized solar cells. Applied Surface Science, 2013, 277, 231-236.	6.1	30
83	Low temperature electrochemical deposition of nanoporous ZnO thin films as novel NO2 sensors. Electrochimica Acta, 2013, 90, 530-534.	5.2	59
84	Sn-Doped TiO ₂ Photoanode for Dye-Sensitized Solar Cells. Journal of Physical Chemistry C, 2012, 116, 8888-8893.	3.1	241
85	Phenothiazine–triphenylamine based organic dyes containing various conjugated linkers for efficient dye-sensitized solar cells. Journal of Materials Chemistry, 2012, 22, 25140.	6.7	120
86	Molecular organic conductors with triiodide/hole dual channels as efficient electrolytes for solid-state dye sensitized solar cells. RSC Advances, 2012, 2, 5550.	3.6	5
87	High-Performance Plastic Platinized Counter Electrode <i>via</i> Photoplatinization Technique for Flexible Dye-Sensitized Solar Cells. ACS Nano, 2012, 6, 9596-9605.	14.6	62
88	Electrodeposition of Platinum on Plastic Substrates as Counter Electrodes for Flexible Dye-Sensitized Solar Cells. Journal of Physical Chemistry C, 2012, 116, 2850-2857.	3.1	62
89	Nitrogen-doped graphene as transparent counter electrode for efficient dye-sensitized solar cells. Materials Research Bulletin, 2012, 47, 4252-4256.	5.2	31
90	Influence of the antennas in starburst triphenylamine-based organic dye-sensitized solar cells: phenothiazine versus carbazole. RSC Advances, 2012, 2, 4507.	3.6	43

#	Article	IF	CITATIONS
91	Triptolide inhibits proliferation and invasion of malignant glioma cells. Journal of Neuro-Oncology, 2012, 109, 53-62.	2.9	26
92	Effects of different acceptors in phenothiazine-triphenylamine dyes on the optical, electrochemical, and photovoltaic properties. Dyes and Pigments, 2012, 94, 150-155.	3.7	43
93	"Soggy sand―electrolyte based on COOH-functionalized silica nanoparticles for dye-sensitized solar cells. Electrochemistry Communications, 2012, 16, 10-13.	4.7	26
94	A novel thixotropic and ionic liquid-based gel electrolyte for efficient dye-sensitized solar cells. Electrochimica Acta, 2012, 68, 235-239.	5.2	17
95	Improved photovoltaic performance of dye-sensitized solar cells by Sb-doped TiO2 photoanode. Electrochimica Acta, 2012, 77, 54-59.	5.2	45
96	Triphenylamine-based starburst dyes with carbazole and phenothiazine antennas for dye-sensitized solar cells. Journal of Power Sources, 2012, 199, 426-431.	7.8	83
97	Mono-ion transport electrolyte based on ionic liquid polymer for all-solid-state dye-sensitized solar cells. Solar Energy, 2012, 86, 1546-1551.	6.1	21
98	High conversion efficiency of pristine TiO2 nanotube arrays based dye-sensitized solar cells. Science Bulletin, 2012, 57, 864-868.	1.7	3
99	An iodine-free electrolyte based on ionic liquid polymers for all-solid-state dye-sensitized solar cells. Chemical Communications, 2011, 47, 2700.	4.1	88
100	Targeting oncogenic miR-335 inhibits growth and invasion of malignant astrocytoma cells. Molecular Cancer, 2011, 10, 59.	19.2	113
101	High-performance novel acidic ionic liquid polymer/ionic liquid composite polymer electrolyte for dye-sensitized solar cells. Electrochemistry Communications, 2011, 13, 60-63.	4.7	34
102	Polymer–metal complex as gel electrolyte for quasi-solid-state dye-sensitized solar cells. Electrochimica Acta, 2011, 56, 1605-1610.	5.2	11
103	Conversion enhancement of flexible dye-sensitized solar cells based on TiO2 nanotube arrays with TiO2 nanoparticles by electrophoretic deposition. Electrochimica Acta, 2011, 56, 6184-6188.	5.2	32
104	PEO-imidazole ionic liquid-based electrolyte and the influence of NMBI on dye-sensitized solar cells. Electrochimica Acta, 2011, 56, 6271-6276.	5.2	19
105	Zinc-Doping in TiO ₂ Films to Enhance Photovoltaic Performance of Dye-Sensitized Solar Cells. Applied Mechanics and Materials, 2011, 66-68, 224-228.	0.2	0
106	Photocatalytic activity enhancement of TiO ₂ porous thin film due to homogeneous surface modification of RuO ₂ . Journal of Materials Research, 2011, 26, 1532-1538.	2.6	11
107	Fabrication of high performance Pt counter electrodes on conductive plastic substrate for flexible dye-sensitized solar cells. Electrochimica Acta, 2010, 55, 3721-3726.	5.2	116
108	Preparation and performance of dye-sensitized solar cells based on ZnO-modified TiO2 electrodes. International Journal of Minerals, Metallurgy and Materials, 2010, 17, 92-97.	4.9	38

#	Article	IF	CITATIONS
109	Electrochemical impedance analysis of nanoporous TiO2 electrode at low bias potential. Chinese Chemical Letters, 2010, 21, 959-962.	9.0	13
110	Low temperature fabrication of flexible carbon counter electrode on ITO-PEN for dye-sensitized solar cells. Chinese Chemical Letters, 2010, 21, 1137-1140.	9.0	10
111	Electrodeposition of SnO2 nanocrystalline thin film using butyl-rhodamine B as a structure-directing agent. Chinese Chemical Letters, 2010, 21, 1505-1508.	9.0	4
112	Novel chemically cross-linked solid state electrolyte for dye-sensitized solar cells. Electrochimica Acta, 2010, 55, 5803-5807.	5.2	8
113	Photovoltaic performance improvement of dye-sensitized solar cells based on tantalum-doped TiO2 thin films. Electrochimica Acta, 2010, 56, 396-400.	5.2	156
114	Preparation of nanocrystalline TiO2 thin film at low temperature and its application in dye-sensitized solar cell. Journal of Solid State Electrochemistry, 2009, 13, 651-656.	2.5	43
115	In situ quaterizable oligo-organophosphazene electrolyte with modified nanocomposite SiO2 for all-solid-state dye-sensitized solar cell. Electrochimica Acta, 2009, 54, 4186-4191.	5.2	19
116	Influences of poly(ether urethane) introduction on poly(ethylene oxide) based polymer electrolyte for solvent-free dye-sensitized solar cells. Electrochimica Acta, 2009, 54, 6645-6650.	5.2	28
117	Synthesis of pyridine derivatives and their influence as additives on the photocurrent of dye-sensitized solar cells. Journal of Applied Electrochemistry, 2009, 39, 147-154.	2.9	21
118	Fluorescence and sensitization performance of phenylene-vinylene-substituted polythiophene. Science Bulletin, 2009, 54, 1669-1676.	9.0	10
119	Performances improvement of eosin Y sensitized solar cells by modifying TiO2 electrode with silane-coupling reagent. Science Bulletin, 2009, 54, 2633-2640.	9.0	5
120	Polymer electrolyte using <i>in situ</i> quanternization for all solidâ€state dyeâ€sensitized solar cells. Polymers for Advanced Technologies, 2009, 20, 519-523.	3.2	4
121	Electrophoretic deposition of nanocrystalline TiO2 films on Ti substrates for use in flexible dye-sensitized solar cells. Electrochimica Acta, 2009, 54, 4467-4472.	5.2	80
122	Performance characteristics of dye-sensitized solar cells with counter electrode based on NiP-plated glass and titanium plate. Current Applied Physics, 2009, 9, 1005-1008.	2.4	10
123	Improvements of photocurrent by using modified SiO2 in the poly(ether urethane)/poly(ethylene) Tj ETQq1 1 0. 2009, , 3895.	784314 rg 4.1	BT /Overlock 62
124	Efficiency enhancement of solidâ€state dye sensitized solar cell by <i>in situ</i> deposition of Cul. Surface and Interface Analysis, 2008, 40, 1393-1396.	1.8	5
125	Light harvesting enhancement for dye-sensitized solar cells by novel anode containing cauliflower-like TiO2 spheres. Journal of Power Sources, 2008, 182, 370-376.	7.8	109
126	A new ionic liquid based quasi-solid state electrolyte for dye-sensitized solar cells. Journal of Photochemistry and Photobiology A: Chemistry, 2008, 194, 20-26.	3.9	50

#	Article	IF	CITATIONS
127	The effect mechanism of 4-ethoxy-2-methylpyridine as an electrolyte additive on the performance of dye-sensitized solar cell. Colloids and Surfaces A: Physicochemical and Engineering Aspects, 2008, 326, 42-47.	4.7	20
128	Dye-sensitized solid-state solar cells fabricated by screen-printed TiO2 thin film with addition of polystyrene balls. Chinese Chemical Letters, 2008, 19, 1004-1007.	9.0	4
129	Cauliflower-like TiO2 rough spheres: Synthesis and applications in dye sensitized solar cells. Microporous and Mesoporous Materials, 2008, 112, 45-52.	4.4	30
130	Solidification of liquid electrolyte with imidazole polymers for quasi-solid-state dye-sensitized solar cells. Materials Chemistry and Physics, 2008, 107, 61-66.	4.0	56
131	Room temperature fabrication of porous ZnO photoelectrodes for flexible dye-sensitized solar cells. Chemical Communications, 2007, , 2847.	4.1	97
132	Investigation of PEO-imidazole ionic liquid oligomer electrolytes for dye-sensitized solar cells. Solar Energy Materials and Solar Cells, 2007, 91, 785-790.	6.2	82
133	The use of poly(vinylpyridine-co-acrylonitrile) in polymer electrolytes for quasi–solid dye-sensitized solar cells. Electrochimica Acta, 2007, 52, 4858-4863.	5.2	53
134	The effects of pyridine derivative additives on interface processes at nanocrystalline TiO ₂ thin film in dyeâ€sensitized solar cells. Surface and Interface Analysis, 2007, 39, 809-816.	1.8	45
135	Novel counter electrodes based on NiP-plated glass and Ti plate substrate for dye-sensitized solar cells. Journal of Materials Science, 2007, 42, 5281-5285.	3.7	12
136	Quasi-solid state dye-sensitized solar cells based on pyridine or imidazole containing copolymer chemically crosslinked gel electrolytes. Science Bulletin, 2007, 52, 2320-2325.	1.7	10
137	Preparation of porous nanocrystalline TiO2 electrode by screen-printing technique. Science Bulletin, 2007, 52, 2481-2485.	1.7	11
138	Novel polymer electrolytes containing chemically crosslinked gelators for dye-sensitized solar cells. Polymers for Advanced Technologies, 2006, 17, 512-517.	3.2	21
139	Computer simulations of light scattering and mass transport of dye-sensitized nanocrystalline solar cells. Journal of Electroanalytical Chemistry, 2006, 588, 51-58.	3.8	23
140	A new type quasi-solid state electrolyte for dye-sensitized solar cells. Science Bulletin, 2006, 51, 1551-1556.	1.7	8
141	Preparation of nano-Pt-modified electrode and its electrocatalytic activity investigation. Materials Chemistry and Physics, 2006, 97, 261-266.	4.0	1
142	Sonication–hydrothermal combination technique for the synthesis of titanate nanotubes from commercially available precursors. Materials Research Bulletin, 2006, 41, 237-243.	5.2	53
143	A novel polymer quaternary ammonium iodide and application in quasi-solid-state dye-sensitized solar cells. Journal of Photochemistry and Photobiology A: Chemistry, 2005, 170, 1-6.	3.9	32
144	A novel high-performance counter electrode for dye-sensitized solar cells. Electrochimica Acta, 2005, 50, 5546-5552.	5.2	65

#	Article	IF	CITATIONS
145	Wavelet analysis of the surface morphologic of nanocrystalline TiO2 thin films. Surface Science, 2005, 579, 37-46.	1.9	17
146	Characterization of nanocrystalline porous CdSe thin films by electrolyte electroabsorption spectroscopy. Thin Solid Films, 2005, 479, 188-192.	1.8	8
147	A 7.72% efficient dye sensitized solar cell based on novel necklace-like polymer gel electrolyte containing latent chemically cross-linked gel electrolyte precursors. Chemical Communications, 2005, , 5687.	4.1	73
148	Gel polymer electrolytes based on polyacrylonitrile and a novel quaternary ammonium salt for dye-sensitized solar cells. Materials Research Bulletin, 2004, 39, 2113-2118.	5.2	58
149	Synthesis and ionic conductivity of a polysiloxane containing quaternary ammonium groups. Polymers for Advanced Technologies, 2004, 15, 61-64.	3.2	71
150	X-ray photoelectron spectroscopy analysis of the stability of platinized catalytic electrodes in dye-sensitized solar cells. Surface and Interface Analysis, 2004, 36, 1437-1440.	1.8	29
151	Influence of chemical treatments on the photoinduced charge carrier kinetics of nanocrystalline porous TiO2 films. Journal of Photochemistry and Photobiology A: Chemistry, 2003, 159, 41-45.	3.9	2
152	Light scattering characteristic of TiO2 nanocrystalline porous films. Science Bulletin, 2003, 48, 856.	1.7	4
153	Local conductivity study of TiO2 electrodes by atomic force microscopy. Surface and Interface Analysis, 2001, 32, 125-129.	1.8	6
154	Studies on the interfacial charge transfer processes of nanocrystalline CdSe thin film electrodes by intensity modulated photocurrent spectroscopy. Science in China Series B: Chemistry, 2000, 43, 443-449.	0.8	4
155	Femtosecond Time-Resolved Near-Field Spectroscopy of CdSe Nanocluster Films. Chinese Physics Letters, 1999, 16, 683-685.	3.3	1
156	Photoelectrochemical studies of H2 evolution in aqueous methanol solution photocatalysed by Q-ZnS particles. Journal of Photochemistry and Photobiology A: Chemistry, 1999, 125, 135-138.	3.9	7
157	Characterization of TiO2 nanocrystalline thin film by scanning tunneling microscopy and scanning tunneling spectroscopy. Applied Surface Science, 1999, 143, 169-173.	6.1	14
158	Scanned laser spot photocurrent response studies of surface modifications of CdSe thin film electrodes. Applied Surface Science, 1995, 90, 321-324.	6.1	0